Electronic Supplementary Material (ESI) for Journal of Materials Chemistry A.

Supporting Information

$HC(NH_2)_2PbI_3$ as thermally stable absorber for efficient ZnO-based perovskite solar cells

Jiaxing Song[a], Weidong Hu[b], Xiao-Feng Wang[b]*, Gang Chen[b], Wenjing Tian[a,b]* and Tsutomu Miyasaka[c]

[a] State Key Laboratory of Supramolecular Structure and Materials, Jilin University, Changchun 130012, PR China

[b] Key Laboratory of Physics and Technology for Advanced Batteries, Ministry of Education, College of Physics, Jilin University, Changchun 130012, PR China

[c] Graduate School of Engineering, Toin University of Yokohama, 1614 Kurogane-cho, Aoba, Yokohama, Kanagawa225-8503, Japan

E-mails: xf_wang@jlu.edu.cn(X.-F. Wang) and wjtian@jlu.edu.cn (W. Tian)

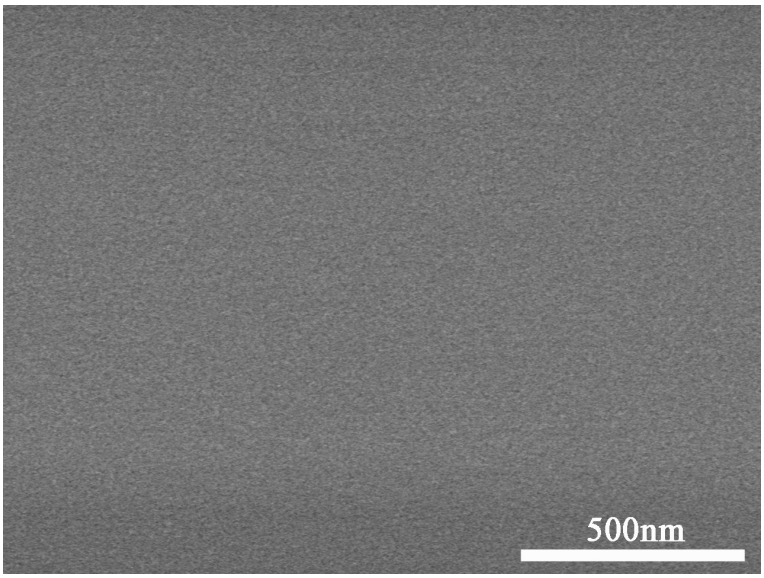

Figure S1. High magnification surface SEM image of ZnO nanoparticle thin film on ITO.

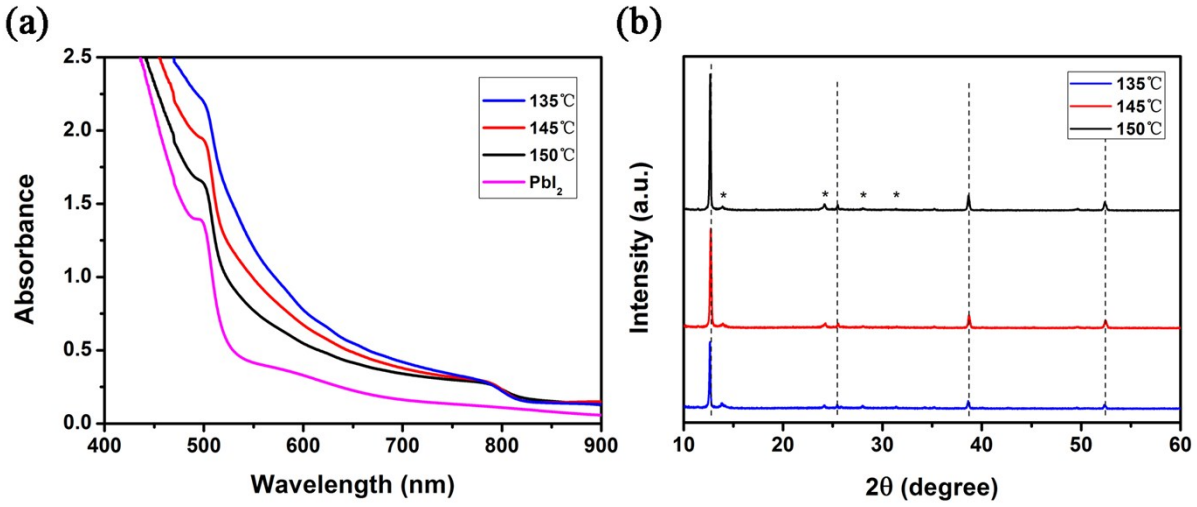

Figure S2. (a) UV-vis-NIR absorption spectra and (b) X-ray diffraction patterns of $FAPbI_3$ thin films with different annealing temperature. Dashed lines denote the PbI_2 diffraction peaks and asterisks denote that of $FAPbI_3$.

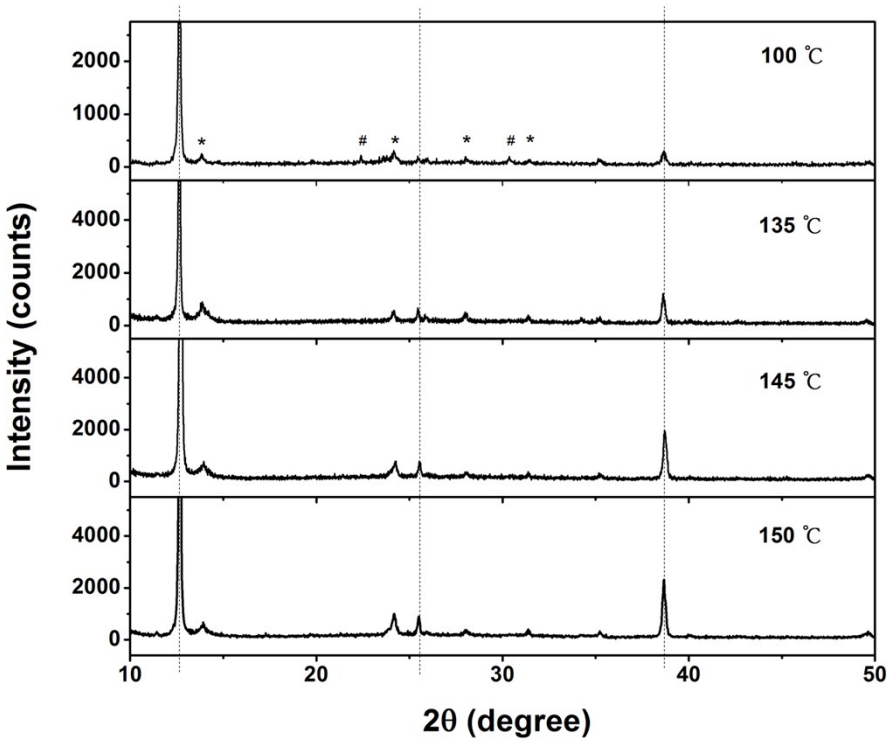

Figure S3. X-ray diffraction patterns of $FAPbI_3$ thin films with different annealing temperature. Dashed lines denote the PbI_2 diffraction peaks, asterisks denote that of black polymorph and octothorpes denote that of yellow polymorph of $FAPbI_3$.

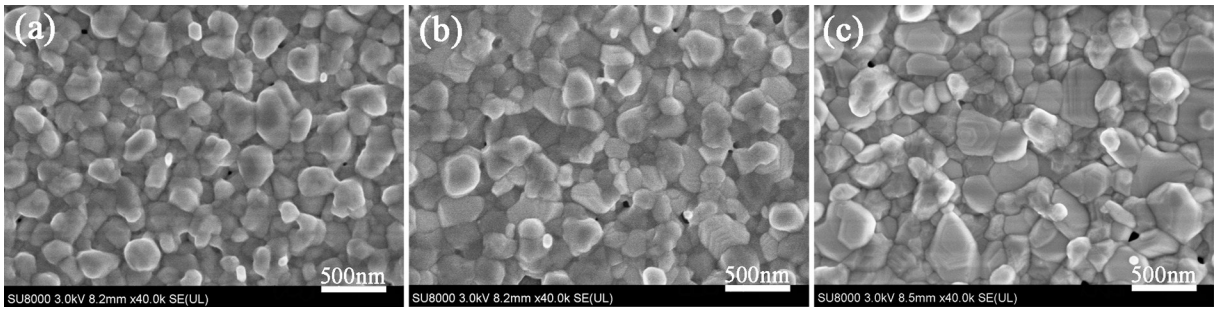

Figure S4. SEM micrographs of ITO/TiO_2/$FAPbI_3$ thin films with different annealing temperature (a) 145°C, (b) 165°C, (c) 185°C.

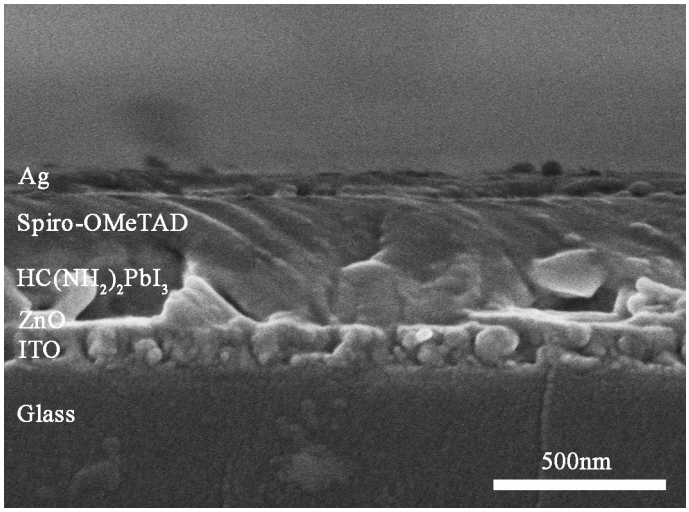

Figure S5. Cross-sectional SEM image of a PSC device based on ZnO.

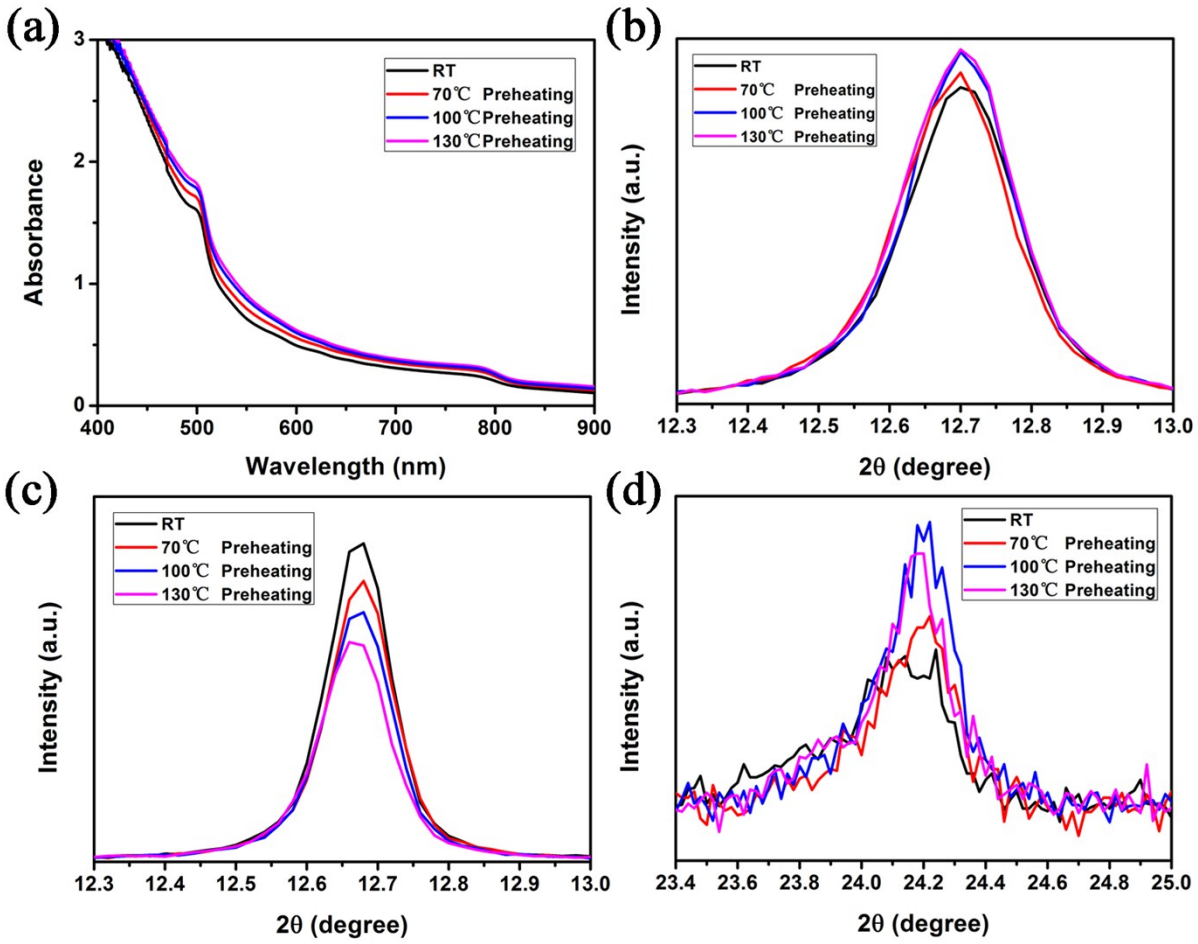

Figure S6. (a) UV-vis-NIR absorption spectra of $FAPbI_3$ thin films obtained from the PbI_2 layers with different preheating temperature. The enlarged X-ray diffraction patterns of ITO/ZnO/PbI_2 films at 2θ =12.70° (b) and correspondingly formed ITO/ZnO/$FAPbI_3$ films at 2θ=12.68° (c) corresponding to the PbI_2 layers with different preheating temperature. (d) the enlarged X-ray diffraction patterns of ITO/ZnO/ $FAPbI_3$ films at 2θ =24.2°.

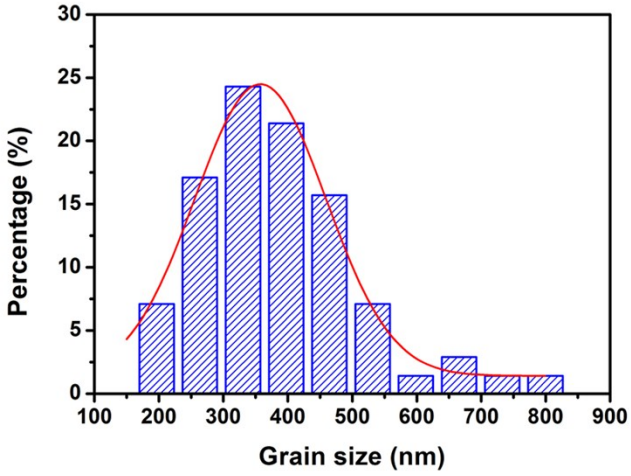

Figure S7. Grain size distribution of the SEM image in Figure 5(c).

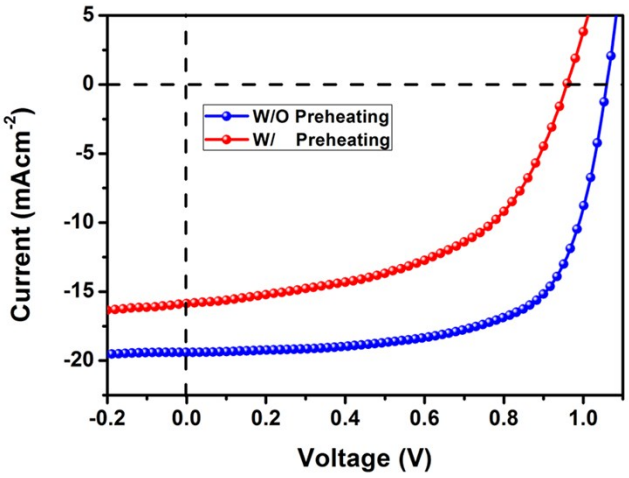

Figure S8. *J-V* characteristic of the ITO/ZnO/$MAPbI_3$/spiro-OMeTAD/Ag devices based on the PbI_2 layers without and with preheating process, respectively.

Table S1. The corresponding photovoltaic performance parameters for PSCs in Figure S8.

Preheating PbI_2	V_{oc} / V	J_{sc} / $mAcm^{-2}$	FF / %	PCE / %
W/O	1.06	19.4	67.1	13.8
W	0.96	16.1	52.3	8.08

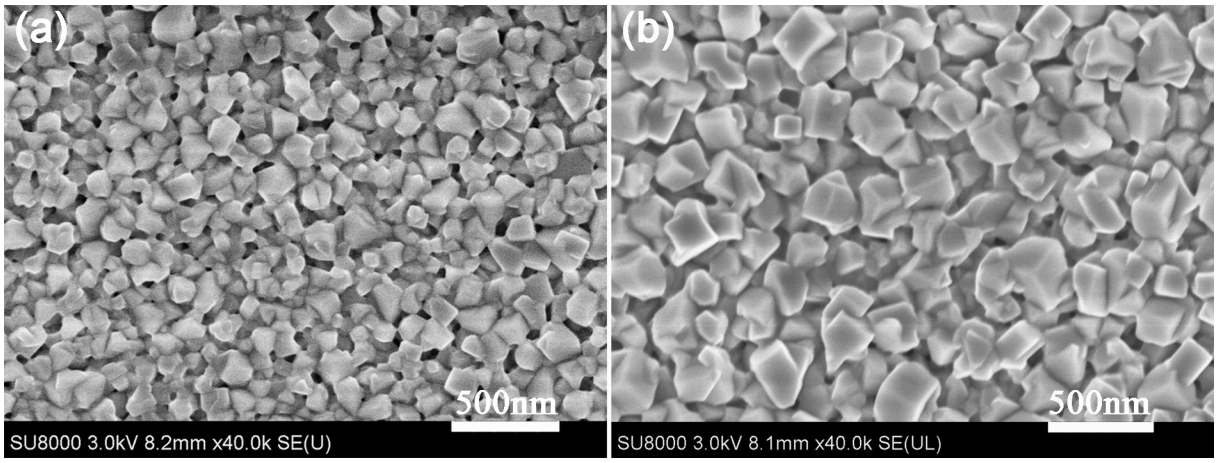

Figure S9. SEM micrographs of ITO/ZnO/$MAPbI_3$ thin films prepared from PbI_2 layers (a) without and (b) with preheating process, respectively.

Table S2. Fitting parameters for EIS data acquired in the dark.

Preheating Temperature (°C)	R_s (Ω)	R_{co} (kΩ)	R_{rec} ($\times 10^4$Ω)	C_{co} (F)
RT	80	68	156	2.45E-8
70	70	62	168	2.72E-8
100	65	58	177	2.95E-8
130	60	57	173	3.03E-8

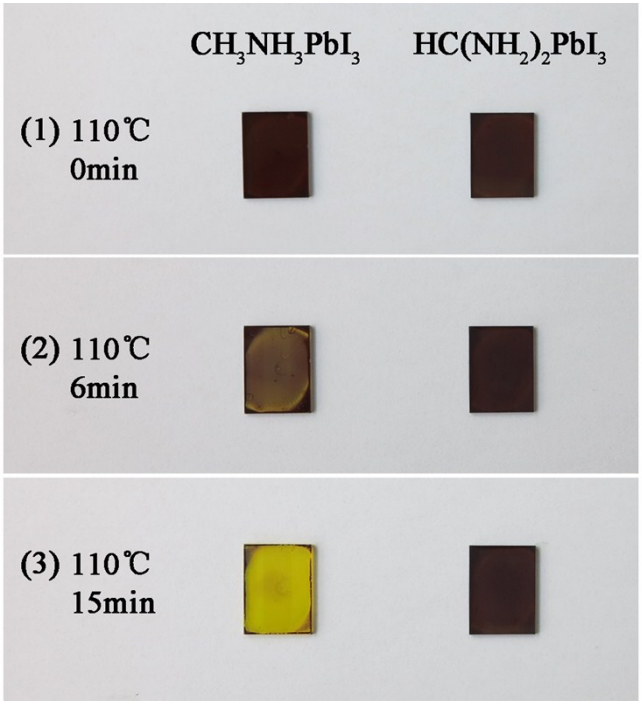

Figure S10. The thermal stability test for ITO/ZnO/$MAPbI_3$ and ITO/ZnO/$FAPbI_3$. (1) 110°C, 0 min (2) 110°C, 6 min (3) 110°C, 15 min.

Table S3. The photovoltaic parameters and the mean values with standard deviations derived from eight cells.

	J_{sc} / mAcm^{-2}	V_{oc} / V	FF	PCE / %
1	20.86	1.08	0.710	16.0
2	20.22	1.09	0.704	15.52
3	20.60	1.08	0.691	15.37

4	20.92	1.08	0.713	16.11
5	21.33	1.07	0.698	15.93
6	21.15	1.06	0.685	15.36
7	20.47	1.07	0.719	15.75
8	20.68	1.06	0.708	15.52
Average	20.78	1.07	0.704	15.70
STDEV	0.37	0.01	0.011	0.29

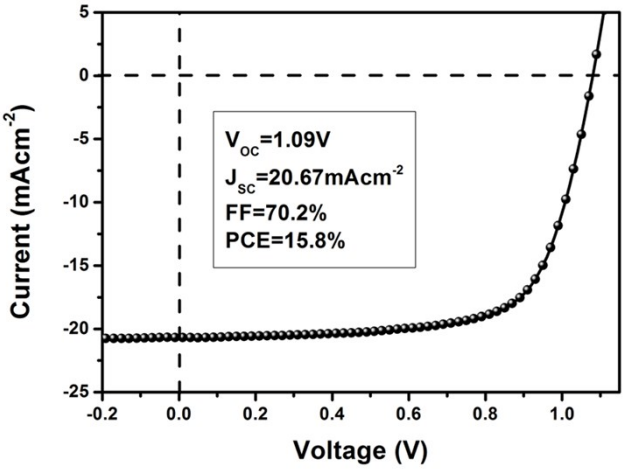

Figure S11. The *J-V* characteristic of the best-performing device with 0.09 cm^{-2} active area measured at 100 $mWcm^{-2}$ AM 1.5G illumination.

Table S4. The photovoltaic parameters and the mean values with standard deviations derived from eight cells with 0.09 cm^{-2} active area.

	J_{sc} / $mAcm^{-2}$	V_{oc} / V	FF	PCE / %
1	19.90	1.10	0.706	15.45
2	20.68	1.06	0.685	15.03
3	20.67	1.09	0.702	15.82
4	20.37	1.08	0.678	14.92
5	20.95	1.09	0.689	15.75

6	20.29	1.08	0.708	15.52
7	20.47	1.07	0.691	15.14
8	20.80	1.07	0.695	15.47
Average	20.51	1.08	0.694	15.39
STDEV	0.33	0.01	0.011	0.33

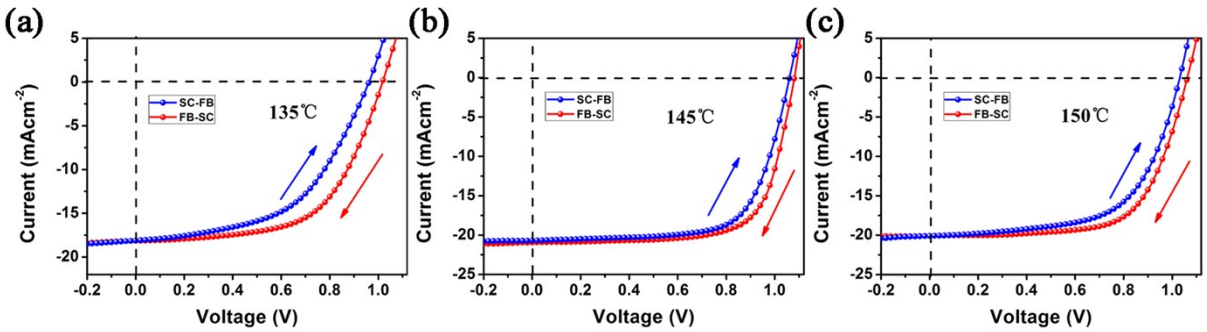

Figure S12. The *J-V* characteristic of the devices measured at 100 mWcm^{-2} AM 1.5G illumination under different scanning directions.

Table S5. The corresponding photovoltaic performance parameters for PSCs in Figure S12.

Annealing temperature		V_{oc} / V	J_{sc} / mAcm^{-2}	FF / %	PCE / %
135	forward	0.96	18.1	52.2	9.0
	back	1.02	18.2	58.9	11.0
145	forward	1.06	20.7	68.6	15.0
	back	1.08	20.9	71.3	16.1
150	forward	1.03	20.1	60.9	12.6
	back	1.06	20.1	66.2	14.1